



Shear walls optimization in a reinforced concrete framed building for seismic risk reduction[☆]

Giulia Cerè^{a,*}, Yacine Rezgui^b, Wanqing Zhao^c, Ioan Petri^b

^a EDF Energy, Hinkley Point C, Bridgwater, TA5 1UD, UK

^b BRE Trust Centre of Sustainable Engineering, School of Engineering, Cardiff University, Cardiff, CF24 3AB, UK

^c School of Computing Sciences, University of East Anglia, Norwich, NR4 7TJ, UK

ARTICLE INFO

Keywords:

Reinforced concrete
Shear walls
Optimization
Risk
Seismic hazards

ABSTRACT

Seismic hazards represent a permanent threat to buildings. The paper argues that risk-oriented approaches provide an interesting solution to account for the long-term resilience of buildings, both for the design of new structures and the rehabilitation of existing ones. The proposed research draws upon the standard definition of risk as a function of vulnerability, hazard and exposure to develop an optimization-based methodology for risk appraisal of buildings in seismic conditions. The proposed methodology allows to identify the optimum layout and thickness of shear walls in a reinforced concrete frame, based on a target risk performance. This is achieved through the coupling of an evolutionary computing environment with an object-oriented structural analysis tool, involving its native Application Programming Interface (API). The latter allows to automate the search for the optimum shear wall configuration solution. The research is validated on the Beichuan Hotel building in Old Beichuan (China), heavily affected by the 2008 Wenchuan Earthquake. The paper evidences that the adoption of the proposed methodology leads to a risk reduction of about 80% compared to the as-built scenario, with additional benefits from both a financial and building functionality perspective.

1. Introduction

Seismic events represent a significant threat to our built environment in earthquake prone areas, putting at risk occupants' lives, while challenging disaster management policies [1–3]. To account for the multiplicity of governing factors that impact on seismic performance across an asset lifecycle, the concept of risk-based design has been introduced [1,4]. For this reason, risk-oriented methodologies are often a preferred preventive strategy for governments as they encompass a wider range of objectives and account for a broader spectrum of factors [5], such as the consideration of the relative importance of a structure over others [1]. This clearly enables an informed implementation of disaster management strategies as well as regulatory frameworks leading to a more efficient resource allocation [6].

The relevance of risk-oriented approaches is critical especially in countries where renovation of existing buildings should be prioritized over new construction programs. In these contexts, reducing the vulnerability of existing constructions is a primary concern given their compliance to older regulatory frameworks [1]. However, few regulatory systems can rely on a systematic risk classification. The first country to integrate a seismic risk classification for buildings has been Italy with the introduction of a system to

[☆] This research is supported by the Building Research Establishment (BRE) and the Natural Environment Research Council (NERC) under grant NE/N012240/1.

* Corresponding author.

E-mail addresses: giulia.cere@nnb-edfenergy.com (G. Cerè), rezgui@cardiff.ac.uk (Y. Rezgui), W.Zhao2@uea.ac.uk (W. Zhao), petri@cardiff.ac.uk (I. Petri).

calculate expected annual losses (EAL) which eventually led to the Sismabonus initiative [7]. The latter entails the provision of tax reductions to those who need to carry out performance enhancement interventions [8]. This initiative has been further integrated in its latest version to include a seismic risk classification for buildings [9].

As a matter of fact, vulnerability assessment alone does not suffice, as being element-specific and therefore targeting only the performance of the structure [1]. Furthermore, vulnerability assessment does not factor in the human and political aspects of seismic emergency, namely disaster management policies. In the context of risk-based methodologies, vulnerability therefore becomes a variable for the final quantification of risk, which is much more comprehensive as it also accounts for the strategic importance of a structure [1,10]. Clearly, the concept of risk finds an effective application in large-scale areas ranging from urban, regional, to national level. This is due to its consideration of relative importance of some structures over others as a result of the specific vulnerability in terms of human lives at stake. For these reasons, strategical buildings generally include schools, hospitals, fire stations or large critical infrastructures, which in case of failure would cause critical disruptions and long-lasting consequences (e.g., power plants) [11,12].

Nonetheless, despite the flourishing research work around the topic, only a few provide concrete implementations of risk into standard practice to mitigate the impact of seismic hazards to buildings. In addition, existing approaches still rely on static methodologies which do not fully exploit current technological advances in terms of optimization techniques. To mitigate the risk for structures to undergo structural consequences in the aftermath of a seismic event, it is necessary to compare different rehabilitation techniques in terms of required costs and generated benefits. Moreover, if a specific rehabilitation technique is selected, optimization can be adopted to find the optimum parameters to attain the desired performance enhancement or specific level of risk.

However, current research does not provide such tools as optimization strategies for performance rehabilitation of buildings and risk-based approaches are dealt with separately. Drawing on the above, this paper will introduce a methodology which systematically integrates an optimization strategy for building rehabilitation into a risk-based framework. Shear walls are chosen above other techniques for seismic rehabilitation of buildings given their frequent integration [13,14] in both new and existing structures compared to other strategies, which are instead limited to post-disaster interventions (e.g., Fibre-Reinforced Polymers strips). Similarly, the application of optimization techniques on shear walls provides a more generic approach than one for instance based on seismic dampers, where the calibration is very specific of the technique itself and does not allow any margin of geometric or layout flexibility.

The analysis will be performed in retrospect in order to compare how damage could have been averted if risk had been accounted for in the initial design stage. A Reinforced Concrete (RC) frame located in Old Beichuan (China) is adopted as a case-study structure and the 2008 Wenchuan earthquake is used as the seismic hazard event to validate this methodology.

In light of the above, this research will provide the following contributions to the body of knowledge:

- A numerical assessment of risk applied to earthquake hazards.
- A novel methodology to quantify the seismic risk of RC structures. This is applicable both at the building level but it can also be scaled up to a district or wider city by factoring in the strategic relevance of the structure.
- A structural enhancement approach to inform (a) the design of RC frames featuring shear walls and (b) structural retrofitting strategies of buildings affected by earthquakes.
- A methodology to identify the optimum shear walls layout and geometrical features given a target risk value.

This paper is structured into 7 sections. A background of existing research regarding risk, optimization strategies for shear-walls and damage evaluation in buildings is presented in Section 2. The proposed formulation for risk adopted in this research is proposed in Section 3, whereas Section 4 provides an overview of the methodology. The results and concluding remarks of this work are elaborated in Sections 5 and 6, respectively.

2. Related work

This section summarizes the state-of-the-art in risk research and applications pertaining seismic hazard analysis. Given the tight relationship between risk and vulnerability, the ensuing subsections will focus on how to quantify damage in buildings from a seismic perspective. Finally, an overview of existing optimization-based strategies for shear walls design for both new and retrofitted buildings is proposed.

2.1. Existing models of risk for buildings

Risk is defined as the combination of hazard, exposure and vulnerability [15] as presented in Equation (1). Each of the composing features has to be individually characterized. To do so, the definitions proposed by the United Nations Office for Disaster Risk Reduction (UNISDR) [16] are herein presented.

$$R_{ke}|_T = |(H_k \otimes V_e) \otimes E|_T \quad (1)$$

The Exposure E is defined as “the situation of people, infrastructure, housing, production capacities and other tangible human assets located in hazard-prone areas” [16]. Although the purpose of the research might differ, there is agreement around the identification of exposure with physical or non-tangible assets located in hazard-prone areas [17]. Some research apply the concept of risk on school buildings, whereby exposure is defined as the number of pupils enrolled in the school and the physical infrastructure [18]. Similar work limits the elements included in the exposure category to buildings and infrastructures [10,17,19]. Even though the approach adopted in the context of school buildings factors in users, an approach targeting the risk of whole urban centres, and not just a specific typology of building, may be faced with the challenge to factor in the occupants’ variability for different building functionalities.

As a matter of fact, the expected number of pupils in a school building can vary only in a given range for safety (e.g., fire hazards, emergency and evacuation of the building) limitations determined in the design phase. On the contrary, residential buildings can account for a much more significant variability in the number of users with subsequent uncertainty in terms of exposure.

Differently, other research work considers risk as the probability of annual failure in seismic conditions drawing on the use of fragility curves [20]. A similar approach in relation to exposure is also adopted by other research [1] which identify exposure as a function of the building use, occupancy and economic impact of the hazard. However, regulatory indexes pertaining the importance class coefficients for buildings are already devised to account for these variables [11,12].

The Hazard H_k is instead defined as “A process, phenomenon or human activity that may cause loss of life, injury or other health impacts, property damage, social and economic disruption or environmental degradation” [16]. In detail, seismic hazard can also be identified as the probability of occurrence of a specific ground shaking in relation to an earthquake event [21] and its characterization should represent the first step for each risk appraisal. However, different methodologies are available to perform a seismic hazard assessment, such as seismic hazard maps [21]. The latter present the expected moment magnitude or ground shaking intensity based on an expected exposure time T_{SL} (i.e., building’s service life) of 50 years with a 90% probability of non-exceedance (corresponding to a 10% probability of exceedance P_E) [21], as shown in Equation (2).

$$T_R = \frac{-T_{SL}}{\ln(1 - P_E)} = \frac{-50}{\ln(1 - 0.1)} = 475 \text{ years} \quad (2)$$

Other research suggest to employ probabilistic seismic hazard analysis (PSHA) for a more accurate estimation [17,22]. This approach is for instance applied to hazardous facilities in earthquake-prone areas [22]. PSHA is further integrated in software such as CAPRA-GIS (a probabilistic risk calculation software based on Geographical Information Systems) [5,23], which provide the opportunity of understanding the most impacting seismic scenario through a probabilistic combination of different events with the additional advantage of geo-referencing the analysed site [18].

The Vulnerability V_e corresponds to “The conditions determined by physical, social, economic and environmental factors or processes which increase the susceptibility of an individual, a community, assets or systems to the impacts of hazards” [16]. Current state of the art features two main methodologies to assess the vulnerability of buildings, namely macro-seismic and probabilistic approaches [24]. However, existing research [24] highlights that oftentimes the utilization of probabilistic methodologies implies cumbersome calculations and requires a reliable set of information to be used as input to characterize the suitably characterize the building. On the other hand, it is also pointed out how macro-seismic approaches do not suffice when targeting quantitative analyses [24] as they principally provide a qualitative analysis based on a classification of structures and construction technologies, such as EMS-98 [25]. Another classification of vulnerability assessment strategies divides them based on the underpinning methodology: (i) approaches relying on damage appraisal, (ii) expert judgment and (iii) mechanical and analytical methodologies.

To this regard, Braga et al. [24] propose a hybrid methodology to assess the vulnerability of existing buildings which combines the macroseismic approach with probabilistic methodologies. Despite the potential for transferability, the difficulties in fetching information such as financial losses hinder the adaptability of this methodology in the Chinese context for the scope of this analysis. On the other side, the seminal work proposed by Lagomarsino and Giovinazzi [26] for the calculation of vulnerability curves relies on a highly accurate set of information (e.g., soil parameters) which are not available in this analysis.

While hazard and exposure are respectively site and building-specific, vulnerability consists in the only component where it is concretely possible to physically intervene in order to attain a risk reduction. The seismic hazard is in fact characterized based on hazard maps which define the specific acceleration for a selected site of analysis, whereas exposure is defined at the district scale as the amount of elements at risk. Therefore, the consideration of vulnerability reduction in buildings is often associated to a lower risk. Most approaches tend to address the building’s vulnerability rather than globally encompassing the analysis of seismic risk. It is however acknowledged that vulnerability represents the component where the highest margin of action is attainable. Conversely, exposure varies upon to the number of elements at risk in terms of inhabitants and physical assets. Specifically, regarding the latter, a building’s service life can have an impact on its exposure. Conversely from the others, the quantification of hazard is purely site-specific, hence its influence on seismic risk is constant regardless of vulnerability and exposure.

In correlation to risk assessments, research also considers the financial impact both in terms of disruption and refurbishment interventions. This is generally attained by means of the benefit-cost ratio (BCR) which correlates the costs of the intervention following the disruption to its benefits, which are generally quantified in terms of annual average loss (AAL). The AAL is a function of the structure’s vulnerability and it is computed in both the refurbished and original conditions in order to quantify the benefit attained with the intervention. The BCR is therefore attained calculating the ratio between the benefits resulting from the refurbishment and the cost [10,19]. A BCR higher than 1 therefore indicates the feasibility of the intervention.

To this respect, the Italian Technical Norms for Constructions [12] introduced the structural safety ζ_E . This coefficient is defined according to the formulation in Equation (3) as the ratio between the maximum Peak Ground Acceleration (PGA) which the existing structure $PGA_{SLV,E}$ can endure and the design PGA that would be adopted for a new construction $PGA_{SLV,D}$. This coefficient is functional to identify the vulnerability of an existing structure or when its assessment is enforced due to a series of conditions, such as a change of functionality category [12].

$$\zeta_E = \frac{PGA_{SLV,E}}{PGA_{SLV,D}} \quad (3)$$

Concurrently, the Sismabonus [8,9] proposes a classification of seismic risk for buildings drawing upon two possible approaches,

namely defined as conventional and simplified. While the latter draws upon the European macro-seismic classification [25], the conventional approach utilizes the coefficient C_E to attain a classification of seismic risk factoring the average predicted annual loss (PAM).

2.2. Numerical characterization of damage

In order to benchmark the building's performance based on the analysis of authoritative building regulations, the interstorey drift ratio (IDR) is selected as a representative indicator for seismic structural performance (Structural Engineers Association of California [11,12,27,28]). Namely, the IDR represents the relative drift between two subsequent storeys in a building, divided by the storey's height (i.e., interstorey). Compared to the simple node displacement, the IDR provides a more representative picture of the structure's performance by taking into account adjacent storeys.

The IDR is an established indicator of building performance from a regulatory perspective, widely adopted in research [6,29,30]. As an example, De Domenico and Ricciardi adopt IDR amongst other performance indicators to assess the seismic resilience of RC building where tuned-mass dampers in combination with base isolation are installed [31]. Calvi and Ghobarah further adopt the IDR as an indicator for seismic performance of buildings [32,33].

However, the IDR alone is not sufficient when dealing with dynamic analyses as a primary role is played by geometric irregularities. These reflect on the distribution of stiffness and mass in the building and can lead to torsional actions. To evaluate these effects, eccentricity is usually adopted and it is defined as the distance between the centres of stiffness and mass. Eccentricity represents an effective flag for potential torsional phenomena [34]. The latter are in fact generally the result of the torque generated by the distance between the centres of stiffness and mass multiplied by the horizontal action.

2.3. Existing approaches to shear walls optimization

Optimization-based strategies are not novel to structural engineering and specifically for seismic hazards. Existing research, however, tends to focus on the final stage of the design, proposing strategies to optimize the sizing of shear walls section and reinforcement [35,36].

An example can be found in the work by Kaveh and Zakian [37], who have used a Charged Systems Search (CSS) algorithm to investigate the best design for both moment-resisting frames and shear walls. This approach relies on the adoption of *OpenSees* for structural simulation, whereas *MATLAB* is utilized for computational tasks. A similar work is devised by Atabay [36], who employs a genetic algorithm to perform sizing and cost optimization for shear walls in the context of a beamless 13-storey structure.

These approaches are advantageous in the final design stage, where the preliminary sizing has been approved and the detailed calculation has to be carried out. However, preliminary phases are often time consuming given the repetitive tasks entailed by the need of assessing the feasibility of a series of options. This would entail the consideration of several options for shear walls layout in order to establish a balance between functionality (i.e., internal distribution) and overall building performance.

Specifically, when adopting shear walls, whether the aim is retrofitting or new construction design, usually the process of checking the most performing layout is carried out manually by the professional. Existing research however demonstrates that these tasks can be successfully automated, alleviating the professional from the repetitive calculation burden and enabling her/him to focus on more sophisticated tasks.

A noteworthy strategy to optimize shear walls location in tall buildings has been developed using Python and drawing on an evolutionary algorithm enhanced with mutation and crossover techniques [14]. This work however does not involve further consideration of risk for it to be integrated in a bigger scale framework. Similarly, this work lacks an overall performance-assessment of the building in its whole perhaps due to the authors' choice to privilege the computational part over the adoption of a software for structural performance calculation.

In addition, this work targets explicitly tall buildings given the primary role that shear walls play in relation to this structural typology in both seismic and non-seismic conditions (e.g., wind). Nonetheless, these buildings are less subject to other types of irregularities that interest buildings of less consistent elevations, such as residential structures, hospitals, or schools. It is in the authors' opinion that considering tall buildings does not ensure a more comprehensive consideration of the role of shear walls in the context of seismic design as several concurrent factors have to be incorporated. Clear examples are for instance geometric irregularities in height and shape but also in structural elements sections. It is in fact established how these factors contribute to the occurrence of torsional actions by increasing the torque arm between the actions applied in the centres of stiffness and the mass.

Similarly, existing literature features research targeting shear walls layout optimization in the context of tall buildings [38,39]. Despite the innovative work proposed by these papers, no real optimization is performed therefore preventing the large-scale replicability of their proposed framework. Moreover, the research features a manual pre-definition of a series of shear walls layout which is then tested using the proposed algorithms. It is also worth noting that Titiksh and Bhatt [38] adopt the maximum drift ratio as a structural performance indicator. However, the latter is not representative of the actual performance of a seismically impacted building as it does not provide information regarding the compliance of the structure to the strong column-weak beam behaviour. As such, the IDR is to be considered as it provides a clear representation of the relative drift of subsequent stories, hence of the effective deformation of the structural members.

Another approach which is worth mentioning is proposed by Abualreesh et al. [40]. Their research presents a reliability-based optimization approach which utilizes cost and a reliability-index as targets for the optimization of layout and geometry of shear walls. Despite the valuable work presented, the heavy mathematical overarching framework hinders scalability and potential adaptations, making it necessary for the user to manually intervene to adapt the algorithm more often than necessary when relying on an API. Additionally, the consideration of seismic reliability may suffice when dealing with a single structure, but it does not encompass

an urban-scale assessment due to the limited consideration of additional variables related to the context and its interrelations. Moreover, the paper does not take into account building irregularities in a way to be considered as representative given that the latter are negligible in comparison to the overall structure's height.

Overall, it has been observed how there is a tendency to adopt metaheuristic algorithms for optimization tasks addressing shear walls design and overall genetic algorithms are the most employed by existing research. Drawing on the proposed review, it is also highlighted how the combination between machine learning and retrofitting design could further be investigated overcoming the following gaps:

- Lack of consideration of risks into structural design and optimization.
- Consideration of structural simulation software limited to few approaches focussing on detailed shear walls design.

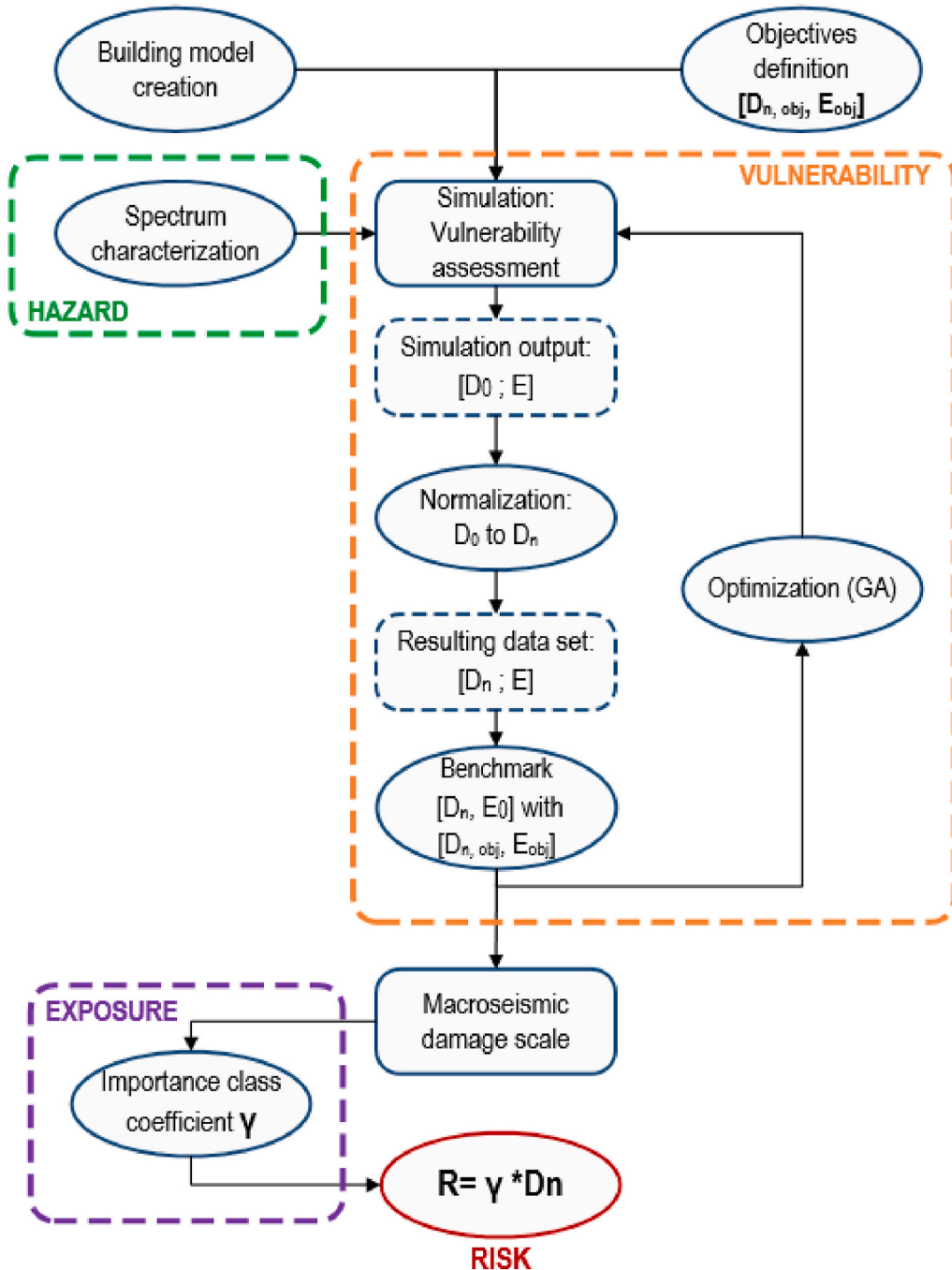


Fig. 1. Integration of risk and optimization strategy. D_n : normalized damage levels, E : eccentricity, $D_{n,obj}$: target normalized damage level, E_{obj} : target eccentricity.

- Limited research on the optimization of shear walls layout.

Based on the gaps identified in the previous paragraph, it is worth highlighting that our research presents a novel approach combining the use of macroseismic scales along with machine learning techniques to optimize the layout of shear walls in RC structures. In addition, our approach binds these aspects to the concept of risk within a holistic framework adopting a performance-based and code-compliant approach in face of seismic hazards.

3. Proposed definition of risk

As formerly introduced in Section 2.1 [15,16], the most adopted definition of risk entails the combination of hazard, exposure and vulnerability. This is reflected in the flowchart presented in Fig. 1 which incorporates the three aforementioned aspects in a workflow featuring the following:

- Preliminary steps:
 - Building model: creation of digital representation of the structure. In the case of the current research, this was attained drawing upon point-cloud data.
 - Objectives $[D_{n,obj}, E_{obj}]$: The normalized damage level D_n and the eccentricity E are defined in value as objectives of the optimization process.
- Core workflow:
 - Hazard: the hazard characterization features the creation of a seismic spectrum.
 - Vulnerability: the evaluation of this aspect starts with the incorporation of the seismic spectrum to perform a structural simulation. The output from the simulation are the values $[D_0, E]$. Subsequently, D_0 is normalized and the dataset D_n is therefore produced. The achieved results for $[D_n, E]$ are benchmarked with the Objectives $[D_{n,obj}, E_{obj}]$ and the optimization process is therefore iterated until the achievement of the latter. The optimization process will be presented more extensively in Section 4.
 - Macroseismic damage scale: The values attained for D_n are functional to define the level of damage within the macroseismic damage scale proposed as part of this research and subsequently outlined in this section.
 - Exposure: This aspect is incorporated by fetching the importance class coefficient depending on the functionality of the structure.
- Risk assessment:
 - The final step utilizes the importance class coefficient and the expected (or experienced) normalized damage level D_n to quantify the risk.

In this research, risk results from the employment of a macroseismic scale which adopts interstorey drift ratio (IDR) as the main indicator for damage. This differentiation is necessary because urban-scale risk entails the consideration of exposure as defined in section 2.1, i.e. the number of elements (i.e., buildings and people) at stake in case of hazard. However, this analysis deals with one building and therefore exposure will be accounted for in a different way as further explored in this section.

In order to adopt an absolute numerical characterization of risk, it is first necessary to start from the identification of damage. As formerly explained, the performance indicator adopted for this research consists in the IDR, normalized based on the minimum and maximum regulatory requirements, as outlined in Section 2.2. This step is functional to achieve values of IDR comprised between 0 and 1 to ease the visualization and appreciation of the results, as well as the final risk assessment. The normalized damage D_n is calculated according to Equation (4), where D_0 represents the original value prior to the normalization.

The maximum and minimum values of IDR respectively corresponding to 2.5% and 0.1% are the highest and lowest thresholds amongst the ones analysed in our literature review [6,29,30,32,33]. Based on the above and the definitions provided in Section 1, D_n therefore can be considered as a quantification of the vulnerability.

$$D_n = \frac{|D_0 - 0.001|}{0.025 - 0.001} \quad (4)$$

The first step towards the characterization of seismic risk is the analytical identification of its three components (i.e., exposure, hazard and vulnerability) [18] as described in the introduction section. At the urban level, exposure can be represented as the number of exposed buildings and their typology. However, this definition cannot be applied when considering risk at the building scale. This discrepancy also applies to vulnerability and hazard given that their integration in the risk model is different, based on whether the scale of analysis is limited to the single building or if it encompasses the urban centre. In fact, when considering the urban level, hazard and exposure can be characterized by respectively referring to hazard maps and building typology. On the contrary, at the building level, hazard is integrated by means of its characterization within the structural behaviour simulation. The building typology is instead factored in through a series of coefficients (e.g., importance class) that further contribute to characterize the hazard and increase the reliability of the analysis.

It is worth noting that within the optimization process highlighted in Fig. 1, the final stage is represented by the “Benchmark” of $[D_n, E]$. This step is crucial to the optimization process as it enables the algorithm to compare - i.e. to benchmark - the values for $[D_n, E]$ achieved within the optimization itself and the objectives. If the objectives are met the cycle terminates and the algorithm can proceed towards the next step.

In light of the above, the formulation for risk at the urban scale can indeed be identified in Equation (1), whereas Equation (5) represents the proposed conceptualization for risk at the building scale. As represented in Equation (5) and in accordance to the above, at the building scale risk is a function of vulnerability, which itself depends on the hazard as in Equation (1).

$$R_{ke}|_T = f|V_c(H_k)|_T \tag{5}$$

In order to further elaborate the proposed formulation for risk, it is relevant to consider the impact of the single building in case of structural failure when scaling up at the urban level. To this regard it can be observed that a heavy structural damage on a strategic building yields to a higher impact on disaster management measures than a residential structure. As a result, when considering the risk at an urban scale, it is not correct to state that the risk of a set of structures simply coincides with the sum of the risks connected to each building.

To factor these considerations in our proposed formulation, the importance class coefficient γ is therefore introduced and Equation (3) is further expanded into Equation (6). Importance classes group buildings in 4 categories according to the consequences of their collapse in terms of human, economic and other type of losses [11]. Eurocode 8 establishes a value of 1 for class II while leaving the others at discretion to the National Annexes. However, the suggested values for classes I, III and IV, respectively, correspond to 0.8, 1.2 and 1.4 [11].

In addition to the above and in order to account for exposure consistently with the definitions provided in section 2.1, the risk at the urban scale is calculated considering the number of vulnerable elements (i.e., structures). This is formalized in Equation (6) through the adoption of a summation operator, where m represents the totality of buildings in a specific urban area. As formerly stated, ensuring the stability of structure considers as a primary objective safeguarding human life. It is therefore relevant to reiterate how this consideration of exposure in terms of buildings, and not people, does not preclude prioritizing people’s safety.

$$R_n = \sum_{i=1}^m \gamma_i \cdot D_{n,i} = \sum_{i=1}^m \gamma_i \cdot \frac{|D_{0,i} - 0.001|}{0.025 - 0.001} \quad \gamma_i = \{0.8, 1, 1.2, 1.4\} \tag{6}$$

Based on the review of regulatory landscape as described in Section 2.2 and the above considerations, a macroseismic scale is developed mainly based on the SEAOC 2000 framework as deemed as the most stringent amongst the reviewed ones (Structural Engineers Association of California [27]). The macroseismic classification aims at identifying levels of building damage corresponding to different benchmark values for IDR and this is presented in Table 1. The transition from damage level to risk is therefore attained through the introduction of the importance class coefficient γ .

It is worth noting that the main difference between R_{n3} and R_{n4} is that the latter combines both permanent and transient damage, hence featuring a higher degree of potential disruption and therefore risk. The lower class R_{n3} , on the contrary, considers the transient and permanent damages separately but also featuring a lower degree of permanent IDR. The transient one exhibits an overlap across the two classes, but R_{n4} considers the permanent and transient IDRs in combination and therefore accounting for a higher D_n .

4. Methodology

This section describes the risk quantification and mitigation methodology suitable for both new (i.e., future) and retrofitted buildings. The methodology leverages existing structural analysis/simulation and calculation tools. Furthermore, the presented methodology draws on the adoption of evolutionary computation techniques and namely of a genetic algorithm to perform optimization tasks.

4.1. Overall research methodology

Prior to detailed description of the different stages of the proposed methodology, an overview of the overarching strategy is given. To this respect, Fig. 2 summarizes the workflow adopted to perform the presented research and the pertaining findings. The proposed methodology is broken down into 3 main stages, as identified in Fig. 2. Namely:

- Stage 1: validation of baseline scenario, presented in §4.2;
- Stage 2: optimization of shear walls height and thickness, presented in §4.3;
- Stage 3: optimization of internal shear walls layout and thickness, presented in §4.4;

Table 1

Damage scale addressing earthquake disruption level to RC structures. R_n : normalized risk, D_n : normalized damage levels, D_0 : non-normalized damage levels.

Risk Level (R_n)	Risk	Damage Level (D_n)	Normalized IDR	Damage Level (D_0)	IDR
R_{n0}	–	D_{n0}	–	D_{00}	–
R_{n1}	$R < 0.05$	D_{n1}	IDR < 3.9% transient Permanent negligible	D_{01}	IDR < 0.2% transient Permanent negligible
R_{n2}	$0.05 < R \leq 0.23$	D_{n2}	$3.9\% < IDR \leq 15.9\%$ transient Permanent negligible	D_{02}	IDR < 0.5% transient Permanent negligible
R_{n3}	$0.23 < R_T \leq 0.78$ $0.05 < R_P \leq 0.23$	D_{n3}	$15.9\% < IDR \leq 55.9\%$ transient (T) $3.9\% < IDR \leq 15.9\%$ permanent (P)	D_{03}	IDR < 1.5% transient (T) IDR < 0.5% permanent (P)
R_{n4}	$0.23 < R \leq 1.34$	D_{n4}	$15.9\% < IDR \leq 95.9\%$ transient and permanent	D_{04}	IDR < 2.5% transient and permanent
R_{n5}	$R > 1.34$	D_{n5}	IDR > 95.9% transient and permanent	D_{05}	IDR > 2.5% transient and permanent

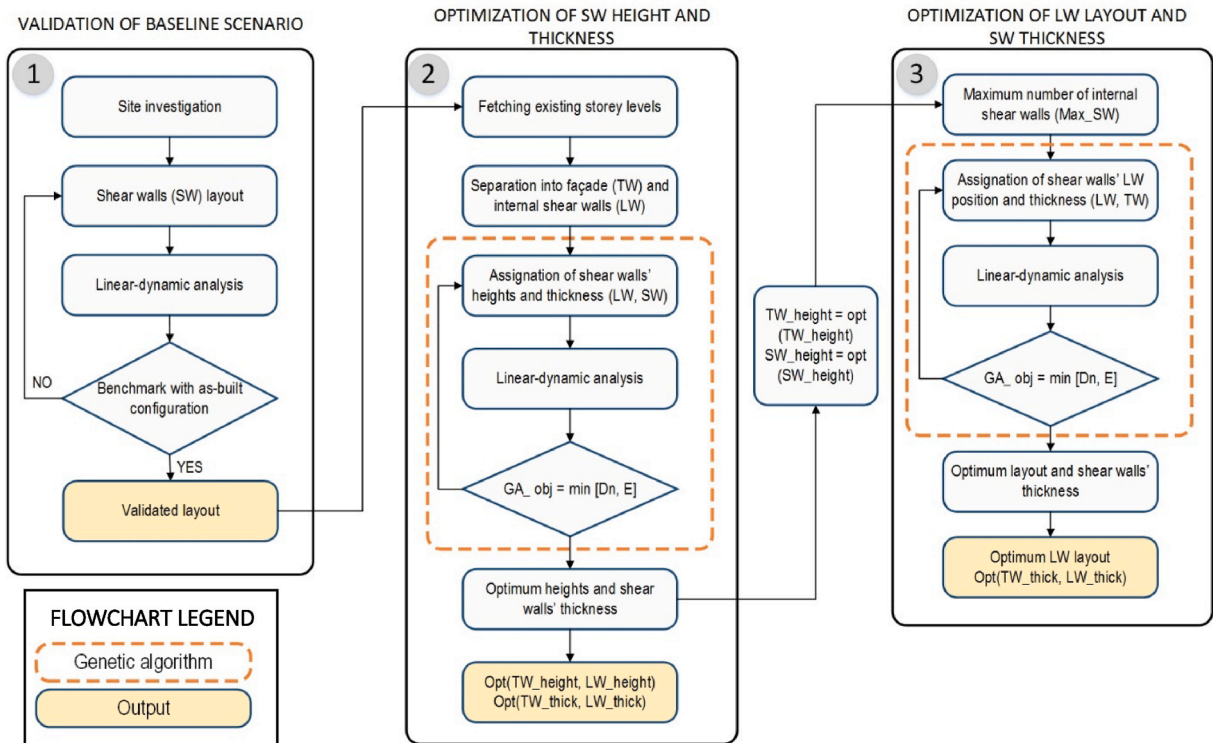


Fig. 2. Proposed methodology. SW=Shear walls, LW = shear walls in façade, TW = internal shear walls, GA = genetic algorithm.

It is worth mentioning the first step to link Matlab to the Robot model is to establish a connection via the COM-based Robot API. This is done drawing on ActiveX technology which allows to import Robot as an object variable into Matlab [41].

The validation stage (i.e., stage 1) is functional to establish the as-built layout of shear walls to then produce a reliable building model to perform the optimization tasks entailed by the two subsequent stages. The second stage aims at investigating the height and thickness of the shear walls in their as-built configuration. This investigation is motivated by the presence of soft-storey and torsional phenomena at the first floor, which is a clear evidence of an excess of rigidity at the lower storey. The third research stage draws on the optimum shear walls height resulting from the second stage, which is assigned to a portion of the shear walls (TW), while for the others, the optimum configuration (LW) is investigated. Nonetheless, the thickness is also preserved as an additional variable to optimize at this stage.

The algorithm chosen to perform the optimization tasks in the second and third research stages is a genetic algorithm (GA), given its established adoption in engineering applications and the quality of results produced [42]. In order to validate the proposed methodology, a real seismic scenario was employed, namely the 2008 Wenchuan seismic event. This research will also be validated by using a building from Old Beichuan in China as a case study. On a different note, when the analysis entails the adoption of an artificial earthquake, relevant building regulations (e.g., Eurocodes) can be selected and the ground shaking can be characterized accordingly, including through soil typology and site-location.

4.2. Stage 1: validation of baseline scenario

The first stage of the proposed work entails the validation of the layout of shear walls and their hypothesised configuration. In order to best identify the configuration of the shear walls, iterative simulations are conducted, and the deformed building configuration is benchmarked with the BIM model and photographic material to ensure the reliability of the baseline scenario. This process is conducted through a trial and error strategy.

In order to simulate the action of the 2008 Wenchuan Earthquake, the acceleration spectrum for the three directions (i.e., x, y and z) was calculated based on seismometer velocities fetched from the IRIS online database [43]. Once the model has been finalized, linear-dynamic analysis was performed. The choice of this typology of seismic analysis draws on the absence of necessary information to perform a reliable characterization of materials as it would be instead needed in the case of a nonlinear-static (i.e., pushover) calculation.

As previously shown in Fig. 1, the vulnerability assessment initially employs a virtual model of the building which is then processed in a structural behaviour analysis software to perform a simulation of the seismic event. Hazard-related features (H) are embedded in the model in the form of pseudo-spectral acceleration spectrum in order to characterize the ground shaking in all three spatial directions.

4.3. Stage 2: identification of optimum shear walls' height and thickness

The aim for this stage is to investigate the optimum shear walls height that would allow to achieve a specific performance level. A genetic algorithm is adopted to address this scenario as described in Table 2. The first step consists in collecting the storeys' elevations. The index of this array will represent the design variable for the GA. Eccentricity and risk are set as objectives for the optimization.

In order to differentiate the allocation of the heights in the building, shear walls are grouped into two categories depending on their location within the frame. Namely, if located in façade the reference group is LW whereas the others are added into the TW category. Thanks to this categorization, it is therefore possible to investigate which is the optimum height for each of the shear wall groups. Ideally, all the shear walls of the frame could have been individually investigated, although this would have entailed the creation of a significantly high number of variables consequently resulting in a time-consuming analysis. The latter represents, in fact, a criticality for GAs, as also shown in Table 3, and therefore, it is important to balance the amount of design variables with population and generation settings.

Given that the time required by the structural behaviour tool to perform a simulation is on average 220 s (i.e., corresponding to slightly less than 4 min), the GA is configured with a population size of 10 individuals and a generation number of 15. These features have been proven sufficient given that the height options are in total 3 and it has been verified that the algorithm attains the convergence between 10 and 15 generations. In addition, the variable to optimize is an integer number representing the index associated to the specific height to be assigned to the shear walls. Consequently, once that the total amount of combinations between the heights array's size and the 2 shear wall groups (including repetitions) has been calculated, there is no need to oversize the population as the simulation result would not vary.

4.4. Stage 3: investigation on optimum shear wall thickness and internal layout

The scope of the third research stage is to utilize as an input the optimum shear wall height calculated in stage 2 to optimize the layout and thickness of the internal shear walls in order to meet the risk and eccentricity objectives for the optimization. Consequently, both the TW and LW shear wall groups are assigned the optimum height as calculated in stage 2. Their thickness is variable given that it could depend on the number and location of the LW. Whereas TW are fixed in number and position, LW shear walls are variable both in number and layout.

On the other side it is acknowledged that strip windows with partially infilled frames in façade lead to the shortening of the effective length of columns, with a consequent increase in their rigidity and hence increasing the likelihood for fragile failure. However, in this context it is decided to preserve the shear walls in correspondence of the shortest building' edges (i.e., TW) to produce the minimum impact on the façade. Therefore, in order to provide the building with the sufficient level of rigidity in face of the seismic action, the intervention would focus on the optimum number and configuration of the shear walls internally.

Given that the presence of shear walls in the floor plan could hinder the internal functionality of the building, and considering the need for shear walls to be continuous across the building's height, this stage aims at investigating the optimum number and layout for the LW shear walls. The advantage of assessing the optimum internal layout for shear walls lies in the opportunity of evaluating the financial benefits in adopting this case study as a lesson-learned in order to better inform future constructions.

The output of the structural simulation is the maximum registered IDR as well as the storey and structural elements for which that value is attained. Based on the calculated IDR, the potential DL can be fetched from the proposed macroseismic scale.

The methodology proposed herein measures vulnerability adopting a hybrid approach between an analytical assessment of the building and the integration of a macroseismic scale. To do so, a preliminary list of the non-perimetral beams is collected and by acting on the position index of the array, the GA is able to determine at each iteration where to position the shear walls. The user is required to enter the maximum amount of shear walls to be adopted by the algorithm to optimize their layout and thickness.

A bespoke algorithm selects the non-perimetral beams and their object ID is stored into an array where the position index is then used as a variable for the GA to determine the layout of the shear walls. In order to ensure the absence of overlapping in terms of index

Table 2
Genetic algorithm settings. CM = Centre of mass, CS = Centre of stiffness, IDR = Inter-storey drift ratio, E = eccentricity.

Scenario Features	Description
Input variables	Array A containing storeys elevations.
Description	The size of main frame elements (i.e., beams and columns) is investigated without operating on the material features
Number of variables	3: Shear walls height ($Height_{TW}$, $Height_{LW}$), Shear walls thickness (tt)
Design variables	index i of the array A
Constraints	$i \in \mathbb{N}$ and $i \in \{1, 2, \dots, size(A)\}$ $tt \in \mathbb{R}$ and $tt \in \{200 \div 400\}$
GA settings	
Objective	Minimize $ IDR_{GA} - IDR_{REAL} $ Minimize $ D_{C,GA} - D_{C,REAL} $ where $D_C = \sqrt{E_x^2 + E_y^2}$ and $E_x = CS_x - CM_x$, $E_y = CS_y - CM_y$
Number of generations (GA)	15
Population number	10
Average simulation time	220 s
Average optimum number of generations	10–15
Stopping criteria	Displacement discrepancy in x,y and z directions <0.001 cm

Table 3

Results summary. 15* = optimized configuration as per Stage 2 of this research, 15** = as built shear wall configuration.

LW shear walls	TW shear walls	Wall thickness [mm]	Standard deviation σ (per storey)						$\mu Rn \pm \sigma$ (global)		RC volume (m ³)	Normalized BCR
			Rn,x			Rn,y			Rn,x	Rn,y		
			St1	St2	St3	St1	St2	St3				
2	4	248	1.54E-02	3.10E-03	4.35E-02	5.63E-03	5.06E-03	7.76E-03	0.0755 ± 0.0603	0.0117 ± 0.0069	1.23E+05	0.0000
3	4	233	1.48E-02	5.91E-03	9.88E-03	6.91E-03	1.03E-03	6.94E-03	0.0435 ± 0.0221	0.0114 ± 0.006	1.40E+05	0.8997
4	4	400	5.25E-04	8.59E-05	3.61E-04	3.34E-03	5.62E-03	5.48E-03	0.0236 ± 0.0031	0.0172 ± 0.0059	1.69E+05	0.9595
5	4	400	3.09E-04	7.78E-04	1.14E-03	3.22E-03	5.50E-03	5.40E-03	0.029 ± 0.0018	0.017 ± 0.0059	1.86E+05	0.9731
6	4	400	7.07E-04	2.07E-03	2.34E-03	3.15E-03	5.42E-03	5.36E-03	0.0329 ± 0.002	0.0171 ± 0.0059	2.07E+05	0.9819
7	4	332	4.15E-04	2.60E-04	1.03E-03	4.11E-03	4.06E-03	4.33E-03	0.0252 ± 0.0018	0.0248 ± 0.0045	2.33E+05	0.9871
8	4	298	8.58E-04	4.52E-04	2.11E-03	3.38E-03	4.70E-03	4.59E-03	0.0317 ± 0.0027	0.0209 ± 0.0048	2.11E+05	0.9830
9	4	324	1.08E-03	1.29E-03	2.76E-03	3.44E-03	6.05E-03	5.92E-03	0.0315 ± 0.0034	0.0136 ± 0.0066	2.27E+05	0.9860
10	4	295	1.98E-03	3.23E-03	3.41E-03	3.92E-03	3.45E-03	3.69E-03	0.0339 ± 0.0029	0.0257 ± 0.0039	2.52E+05	0.9909
11	4	285	3.43E-04	1.00E-03	1.75E-03	4.60E-03	2.06E-03	2.71E-03	0.0299 ± 0.0036	0.0297 ± 0.0035	2.89E+05	0.9943
12	4	250	1.10E-03	2.74E-03	2.62E-03	3.08E-03	4.07E-03	4.04E-03	0.0346 ± 0.0023	0.0209 ± 0.0041	2.40E+05	0.9892
13	4	322	2.69E-03	1.28E-03	1.75E-03	4.74E-03	2.78E-03	2.76E-03	0.0339 ± 0.0024	0.0298 ± 0.0037	3.34E+05	0.9971
14	4	317	1.15E-03	2.33E-03	2.39E-03	4.40E-03	4.56E-03	4.38E-03	0.033 ± 0.002	0.0261 ± 0.0046	3.60E+05	0.9980
15	4	315	1.89E-03	1.65E-03	7.38E-04	4.34E-03	3.63E-03	3.11E-03	0.0204 ± 0.0029	0.0303 ± 0.0039	4.35E+05	0.9995
15*	4	300	9.09E-04	1.20E-03	1.08E-03	6.20E-03	4.11E-04	3.41E-04	0.0374 ± 0.0011	0.038 ± 0.0043	4.09E+05	1.0000
15**	4	300	4.78E-04	2.32E-03	2.51E-03	5.49E-03	3.28E-03	3.05E-03	0.092 ± 0.0658	0.1523 ± 0.0738	1.21E+05	/

selections, inequality constraints are introduced. Assuming for instance a maximum allowed number of n shear walls, the constraints can be formalized as in Equation (7). The equation is then translated into matrix form as in Equation (8) in order for it to be adopted in the GA.

$$x_{n+1} - x_n \leq -1 \quad (7)$$

$$\begin{bmatrix} 1 & -1 & 0 & \dots & 0 & 0 \\ 0 & 1 & -1 & \dots & 0 & 0 \\ \vdots & \vdots & \vdots & \dots & -1 & 0 \\ 0 & 0 & 0 & \dots & 1 & -1 \end{bmatrix} x \leq - \begin{bmatrix} 1 \\ 1 \\ \vdots \\ 1 \end{bmatrix} \quad (8)$$

At each iteration the LW created in the former one are removed and the algorithm introduces a new set of LW according to the process presented in Fig. 3. The total amount of LW for each configuration is represented by $nvars$ and each shear wall is created as a new object first defining its univocal object number $objNumber$. The optimum locations for the LW to be placed at each iteration is identified by the beams pertaining to the span where the wall has to be placed. Therefore $beam_ref$ is an iteration-specific array where the GA stores the object numbers of the beams corresponding to the spans which will host the new LW.

Any wall element in Robot is defined by a contour made of 5 points where the start and end nodes coincide in order to identify a closed perimeter. Therefore, the start node SN and end node EN of the beams are fetched querying the object-specific properties. Only X and Y coordinates are stored as Z is 0 as a default for points 1,2 and 5 of the wall contour as visible in Fig. 3. The Z coordinate for the 2 points defining the top segment of the wall contour (i.e., 3 and 4) is taken from the $highest_slab$ variable. The latter is the result of a preliminary identification of the highest slab of the frame in order to provide continuity of the shear walls throughout the building's elevation averting the structural failures experienced in the as-built scenario. Once the points are created and stored into an

For_Loop to be repeated between i=1 to number of variables (nvars) -1

Assign random available ID **objNumber** to new shear wall
Grab the value for i from the array of

Grab the beam's start node **SN** (first point of shear wall panel contour) from the object

Nodes

Grab the beam's end node **EN** (second point of shear wall panel contour) from the object

Nodes

Extract coordinate X of SN and assign it to **SNx**

Extract coordinate Y of SN and assign it to **SNy**

Extract coordinate X of EN and assign it to **ENx**

Extract coordinate Y of EN and assign it to **ENy**

Create the array points using the Computational Factory tool within Robot.Kernel
'I_CT_POINTS_ARRAY'.

Set the size of 5 elements for the array **points**

Assign the coordinates (**SNx**, **SNy**, 0) for the first bottom edge of the shear wall panel to the first element of **points**

Assign the coordinates (**ENx**, **ENy**, 0) for the second bottom edge of the shear wall panel to the second element of **points**

Assign the coordinates for the first top shear wall panel edge (**ENx**, **ENy**, **highest_slab**) to the third element of **points**

Assign the coordinates for the second top shear wall panel edge (**SNx**, **SNy**, **highest_slab**) to the fourth element of **points**

Assign the coordinates (**SNx**, **SNy**, 0) to the fifth element of **points** to close the panel object

Create shear wall panel contour with ID=**objNumber** and structure of array **points**

Fetch new shear wall **objNumber** from **Objects** and assign it to **wall_obj**

Assign true value to **Meshed** property of **wall_obj**

Assign wall type property to **StructuralType** of **wall_obj** as 'I_OST_WALL'

Assign Label **NameL** for **wall_obj** reinforcement 'I_LT_PANEL_REINFORCEMENT'

Assign Label **WallSectionName** for **wall_obj** thickness 'I_LT_PANEL_THICKNESS'

Assign Label **NameC** for **wall_obj** calculation model 'I_LT_PANEL_CALC_MODEL'

Initialize **wall_obj** object

Add **objNumber** to the existing array of new shear walls panels **New_Walls**

End the Loop

Fig. 3. Pseudocode for the algorithm for shear walls contour modification.

'I_CT_POINTS_ARRAY' object, this is used as an input for the contour with the CreateContour function of the API. The remaining operations to be conducted on the wall pertain to the assignment of labels regarding its thickness, reinforcement provision and calculation algorithm in Robot. These parameters have to be defined prior to the wall creation using the Label object creation and properties assignment [41].

The simulations have been conducted for different shear walls configurations, each of them involving a different number of walls. A number from 2 to 15 longitudinal shear walls (LW) have been considered for a total of 14 simulations. It was decided to range from the minimum possible number of shear walls to a scenario presenting an equivalent number of walls as the as-built configuration. In fact, preserving the initial configuration for the 4 TW in façade, the maximum would correspond to the total of 19 as in the as-built configuration.

In order to select the optimum solutions amongst the results from the different scenarios, the following decision variables have been assessed:

- Maximum D_n for each storey and globally for the whole building;
- Standard deviation of D_n across the storeys and globally to avert changes of behaviour that could lead to local vulnerabilities;
- Eccentricity;
- Layout of LW;
- RC volume adopted as a flag for costs.

Regarding the latter (i.e. RC volume), the volume of material is adopted to represent costs based on the assumption that the price for unit of material is constant, therefore this analysis does not account for discounts based on quantity increments. Any additional cost, such as manpower, transportation and any other site-related cost is also considered proportional to the material with good approximation. In this analysis it is therefore analysed the increase or decrease in cost compared to the baseline rather than the absolute cost of the potential intervention. This is due to the impossibility of retrieving the cost of the initial intervention, therefore an absolute baseline.

To demonstrate the performance and financial benefits resulting from the adoption of this methodology, the BCR adopted by other research [10] is here revised and calculated as follows. The percentage variation is calculated for RC volume, $D_{n,x}$ and $D_{n,y}$ as presented in Equation (9).

$$BCR = \frac{\mu[\Delta D_{n,x}(\%), \Delta D_{n,y}(\%)]}{\Delta C(\%)} \tag{9}$$

The BCR is here the result of the ration of the mean discrepancy between ΔD_n in x and y, and the cost discrepancy ΔC , as shown in Equation (9). The index can clearly vary between negative and positive values considering that the ΔC and ΔD_n could occur as increments or reductions. In order to therefore provide a clearer representation of the BCR, this has been normalized between 0 and 1 based on the maximum and minimum values as calculated in Equation (9).

5. Results

This section is further structured into three subsections. Section 4.1 will firstly present the validation of the baseline scenario and the related shear wall configuration which are then adopted for the ensuing optimization work. Grounding on these findings, Section 4.2 will then present the optimum shear walls height which should have been adopted in order to reduce the damage undergone by the

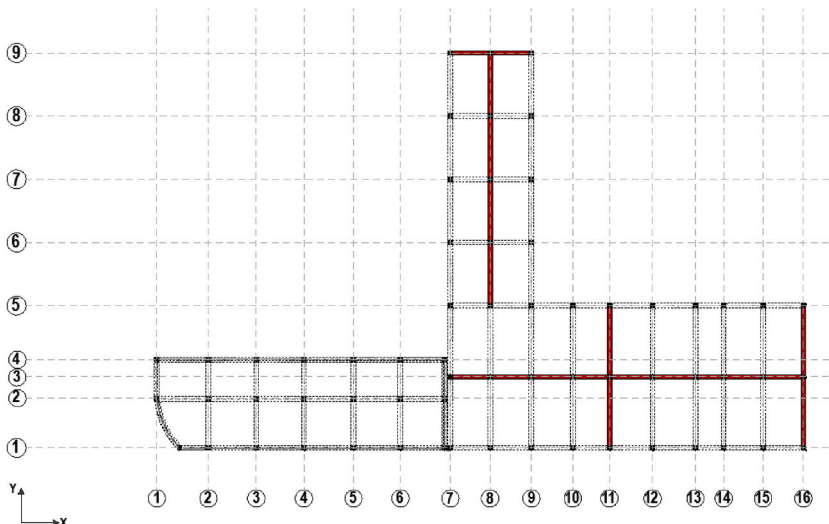


Fig. 4. As-built layout of shear walls.

structure. Finally, building upon the findings from the first two sections, section 4.3 will provide a breakdown of the results obtained to optimize shear walls features and layout for the analysed building.

5.1. Stage 1: validation of as-built shear walls configuration and as-built risk

In order to ensure the reliability of the model adopted to perform the analyses, an initial validation of the model has been performed as outlined in Section 3.1. The as-built shear walls layout is presented in Fig. 4 and it is worth restating how this configuration only applies to the first storey of the structure, as confirmed by Fig. 5a and Fig. 5b. Fig. 5c and d show instead the deformed configuration of the building, which confirms the occurrence of the torsional behaviour, as identified during the site investigation in line with Fig. 5a and b.

Most importantly, Fig. 5c and d illustrate how the torsion is maximum at the junction between the blocks of different elevations, and it almost disappears in coincidence of axis 12. These results are perfectly consistent with the as-built configuration as per Fig. 5a and b where the corresponding column appears to be almost completely un-deformed. Comparing these results with the shear walls layout of Fig. 4, axis 12 appears to be the first axis after the shear walls and this also justifies the lower node displacement undergone by the columns in that position.

Fig. 6 shows instead the average normalized risk calculated according to section 3.2, and relatively to the as-built shear walls layout as presented in Fig. 4. Both in x and y direction, R_n appears to attain its maximum values for axis 7, confirming the post-disaster configuration where the node in correspondence of height discontinuity undergoes the highest displacement. This can be observed by comparing Fig. 5 with the results presented in Fig. 6 specifically concerning the simulation and the as-built damaged configuration. Similarly, the second storey exhibits the highest risk almost throughout the whole frame. This is also consistent with the as-built configuration where the torsional mechanism is initiated in correspondence of the discontinuity and hence affecting first the second storeys.

As it can be observed from Fig. 6a and b, only columns on axes 1 and 3 extend through the second and third storeys. Comparing the results outlined in Fig. 6a and b with the classification proposed in Table 1, and considering the permanent nature of the disruption endured by the structure, it is possible to locate the damage to this building in the fourth category. The algorithm provides the risk based on the formulation presented in Section 3 and since the maximum R_n achieved in the as-built condition is almost 30%, this corresponds to R_{n4} in Table 1. Given the permanent nature of this deformation this cannot be categorized under the R_{n3} risk level.

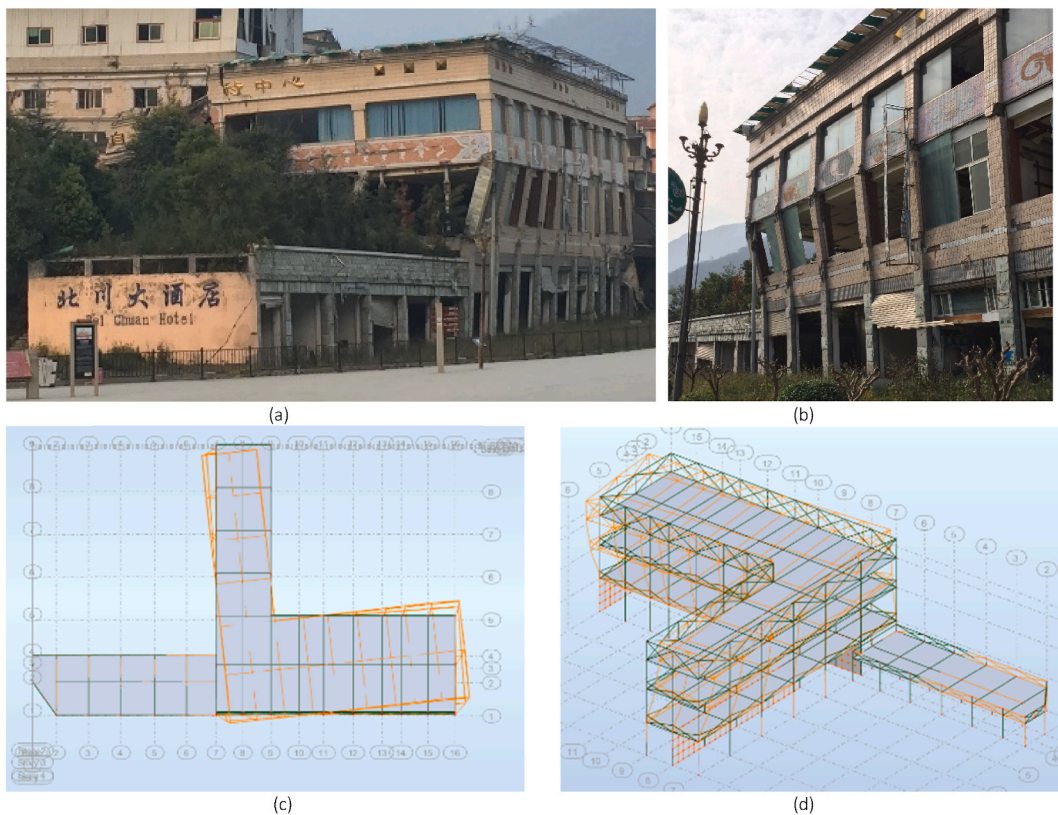


Fig. 5. Beichuan Hotel post-disaster configuration as per site investigations carried out in December 2016 and July 2017 (a)(b) and semantic model with highlighted deformed configuration (b)(c).

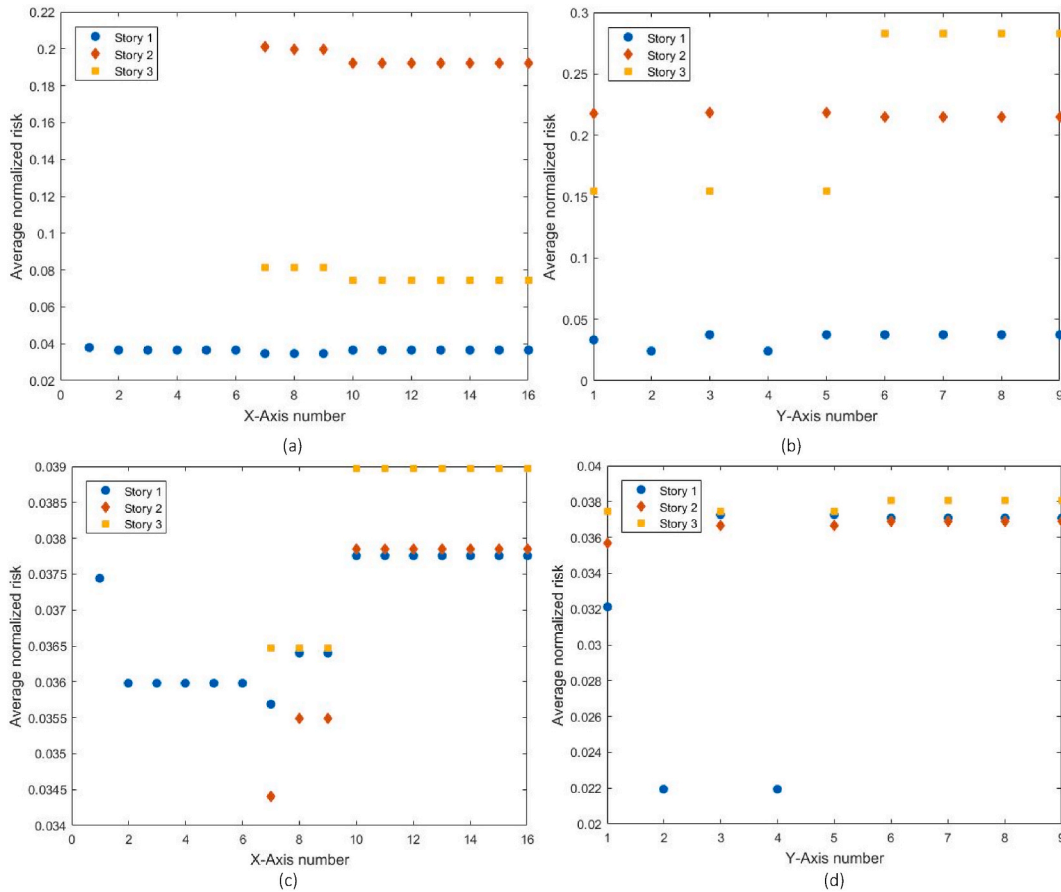


Fig. 6. Average normalized risk across building axes in X (a) and Y (b) direction as per post-damage as-built configuration; Average normalized risk across building axes in X(c) and Y (d) direction with shear walls presenting the as-built configuration but optimized height.

5.2. Stage 2: optimization on shear walls height and thickness

As formerly outlined, this section will address the identification of the optimum height and thickness for shear walls in their initial configuration. The proposed algorithm provides a result consistent with the established requirements for seismically resistant structures, enforcing shear walls to equal the building’s elevation.

The resulting optimum heights for both transversal and longitudinal shear walls correspond in fact to 12.70 m which coincides with the building’s elevation. This result clearly contradicts the as-built shear walls height which corresponds to the first storey of the building. Similarly, it also confirms the validity of this approach but also the improper structural layout adopted in this context at the design stage.

Fig. 6c and d shows in fact a drastic reduction in the normalized risk R_n when comparing it with the as-built results presented in Fig. 6. To this extent, it is relevant to observe how the most significant contribution in terms of risk reduction is exhibited for the second and third storeys. This was predictable given their level of risk and endured damage in the as-built configuration.

Comparing the maximum achieved R_n as presented in Fig. 6c and d with the breakdown proposed in Table 1, it is possible to observe how just the extension of shear walls to the whole building’s elevation leads to a drop in risk and endured damage. Given that the maximum attained R_n corresponds to 3.9% and 3.8% respectively for the X and Y axes, it is possible to locate this new disrupted configuration at the edge between the first and second categories in Table 1. This coincides with a drop in damage of approximately 80% and 86% respectively in X and Y direction. This acquires specific relevance when observing the columns in the first axis for both X and Y given that junction endured the most damage.

Nonetheless, despite the considerable benefit of this optimized configuration, there is a need to highlight the unfeasibility of such solutions in terms of functionality. As a matter of fact, when having a configuration of shear walls such as the one in Fig. 4, extending this to three storeys may become functionally impractical given the fact that these upper levels form the reception of the hotel.

This raises the need to introduce a further level of optimization including the combination of optimum performance and layout which is presented in the next subsection.

5.3. Stage 3: optimization on shear walls thickness and configuration

This section presents the results of the final stage of the methodology, where both the thickness and layout of shear walls are

optimized. This is attained imposing that the shear walls' height equals the building's elevation. Table 3 shows a global overview of the results for each of the options considered. As described in Section 4.4, several parameters have been considered, such as the average R_n both globally and for each storey. The standard deviation σ is also calculated both in terms of the single storey but also for the whole building. Fig. 8 provides instead an overview of the cost and the BCR connected to each option and in accordance to the definitions provided in Section 4.4. These results are analysed in terms of the attained R_n in both X and Y directions and potential cost increase/decrease for each option.

Following to an analysis of the obtained results and an assessment of the solutions in terms of better utilization of the internal space based on the shear walls layout, the selected solution is the 6 LW one. A consideration which is worth highlighting is the preference of the option with 6 LW over the ones with 5 or 4 given the similarity in terms of the performance attained as shown in Table 3. Clearly, the μR_n for all the three options is comparable and so is the error (i.e., variability, standard deviation) for each of them. However, the layout obtained for the solution with 6 LW provides a better utilization of the space.

Similarly, other solutions such as 2 and 3 LW exhibit a higher μR_n compared to the chosen solution, especially for the x direction. In addition, the error in x connected to the average value is considerably higher for those options compared to the one with 6 LW, which physically means a higher variability of vulnerability across the building. Overall, the preferred option exhibits a better uniformity of R_n globally and within the single storeys, meaning that the distribution of stresses is regularized and hence there is less likelihood for occurrence of localised failures.

Fig. 9a shows the distribution of eccentricity values (i.e., cumulative eccentricity for the three building's storey) for the option deemed as the most convenient and performing, namely the configuration with 6 LW shear walls. The correlation between risk and shear wall thickness is shown in Fig. 9b exhibiting a significant improvement compared to the as-built configuration. Similarly can be observed in terms of eccentricity in Fig. 9a, where the overall building eccentricity across the 3 storeys drops from 22.31 m to 5.1 m. Fig. 9b clearly shows how the chosen solution provides both a significant reduction in damage as it can be observed comparing the as-built values for the 3 storeys with the R_n corresponding to the thickness of 400 mm. The R_n values for the optimum shear wall thickness of 400 mm appear in fact compact and not dispersed, confirming the observations above. This demonstrates a better redistribution of stress across the building and structurally averting the occurrence of sudden stiffness changes in the frame which would result in local vulnerabilities (e.g., plastic hinges).

It is relevant to point out that the eccentricity sum has not been shown in Fig. 9 as no significant difference has been attained for this variable across the different options. As a matter of fact, all the options were able to provide 5 ± 0.1 m of minimum eccentricity sum across the storeys with minimum variability across the storeys.

Given the values of R_n attained for the chosen configuration and as shown in Fig. 10, it is possible to confirm that the option with 6 LW shear walls coincides with a R_n1 according to the classification in Table 1. This therefore corresponds to a drop of 3 risk categories compared to the as-built condition.

Fig. 11 further exhibits significant advantages in terms of functionality compared to the option of extending the initial

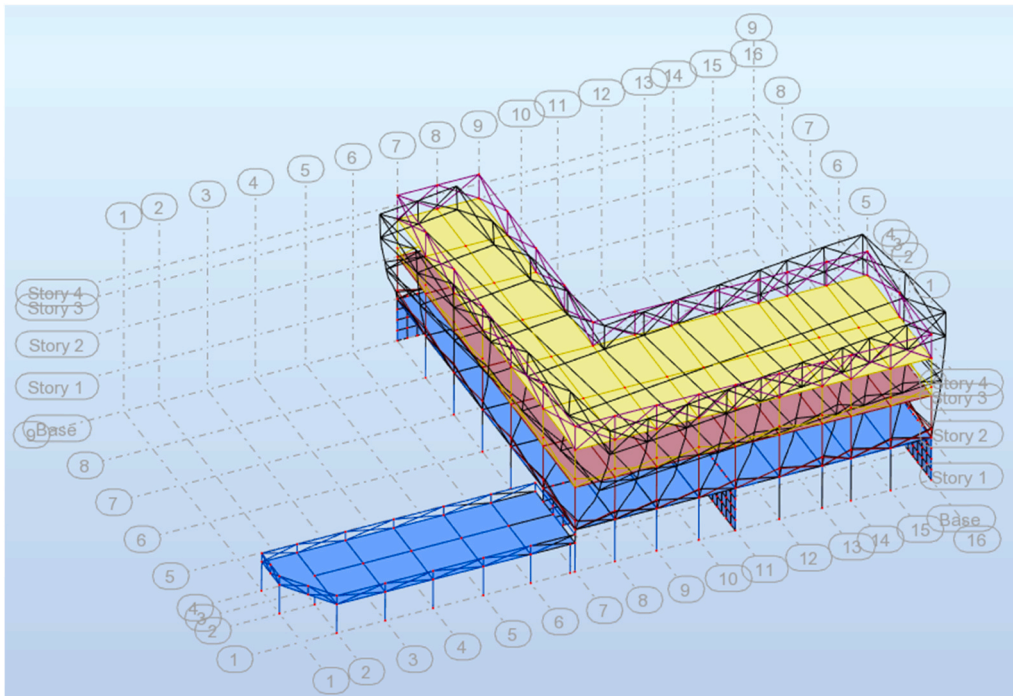


Fig. 7. As-built deformed configuration.

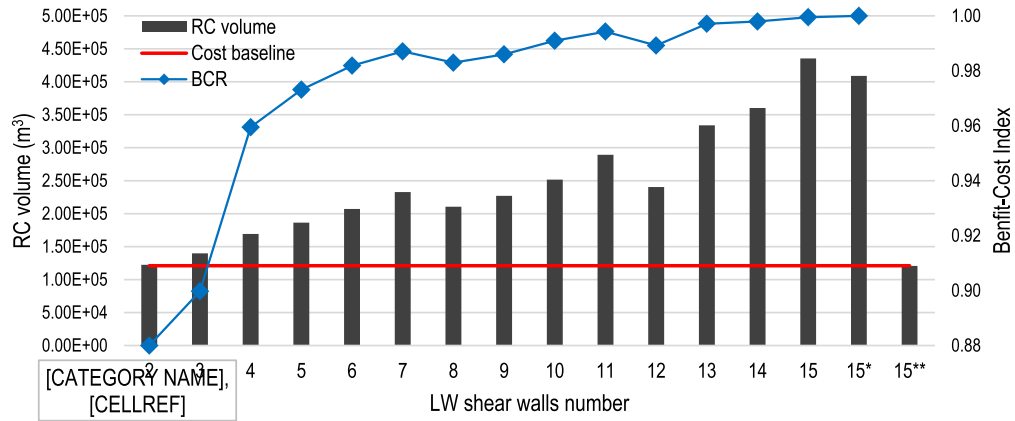


Fig. 8. Overview of the different shear walls configurations and corresponding RC volume and maximum R_n achieved. SW = shear wall, RC = Reinforced Concrete. 15* = optimized configuration as per 2nd stage of this research, 15** = as built shear wall configuration.

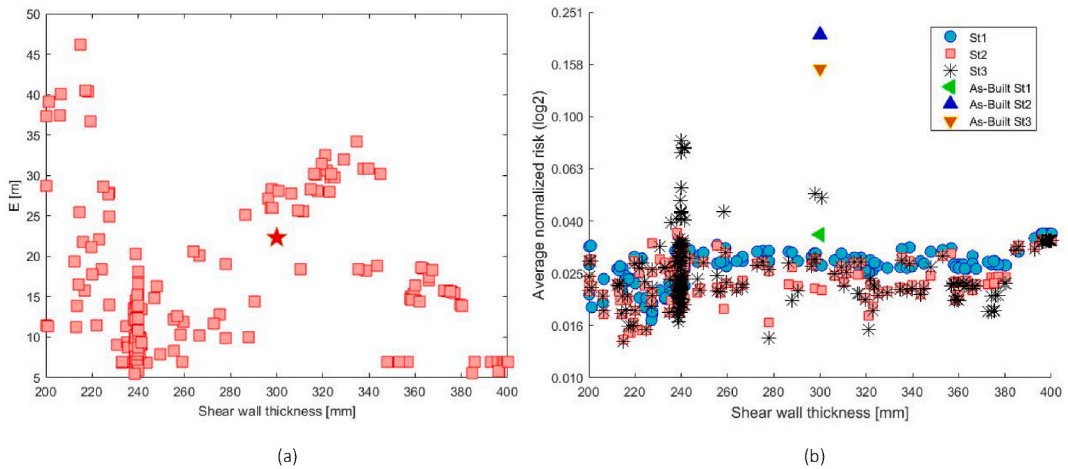


Fig. 9. Eccentricity sum across the storeys for the whole building (as-built eccentricity represented by the red star) (a) and normalized risk (R_n) (b) for the configuration including 6 longitudinal shear walls (LW). (For interpretation of the references to colour in this figure legend, the reader is referred to the Web version of this article.)

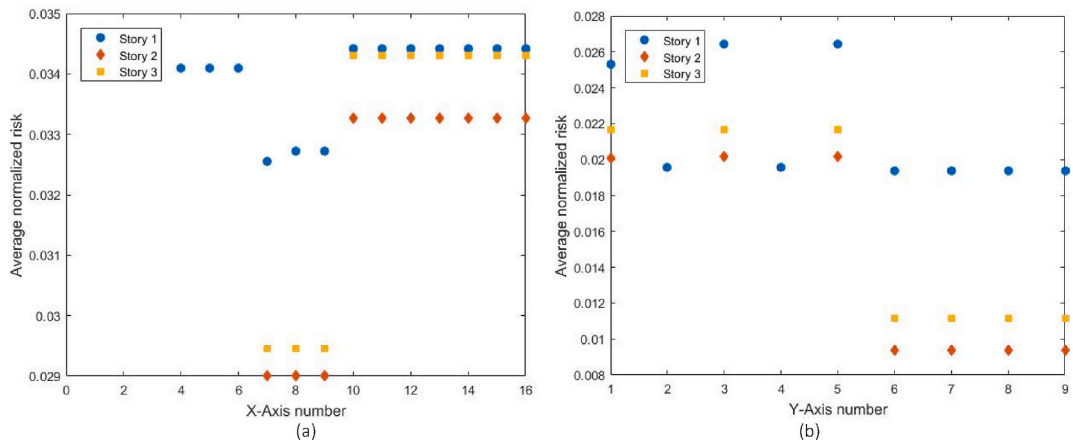


Fig. 10. Normalized risk (R_n) in X and Y direction for the configuration with 6 LW shear walls.

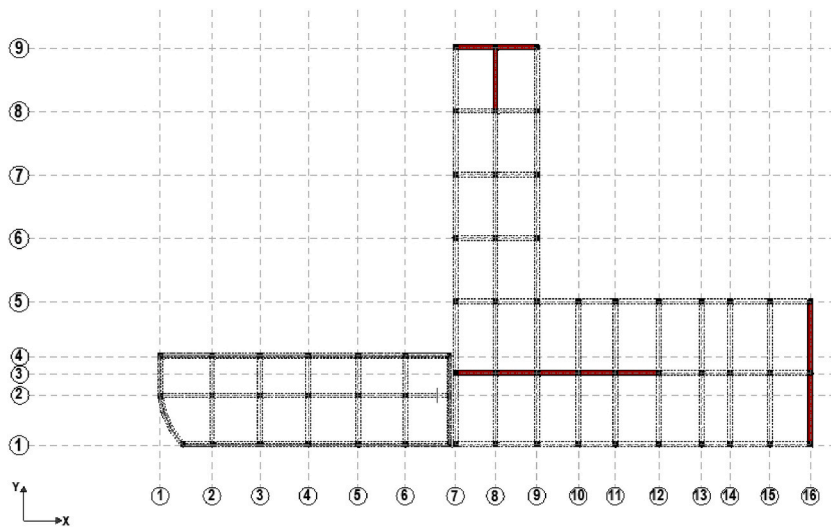


Fig. 11. In-plan distribution of shear walls for the option with 6 LW shear walls.

configuration of shear walls throughout the three storeys. The X-oriented block is in fact provided with a convenient division that would be easily adopted to shield the kitchen and other service rooms from the main reception areas.

6. Discussion

The devised algorithm overall demonstrated that the shear walls height plays a major role in improving the resistance of the structure to seismic actions. In relation to the second stage and comparing Fig. 6c and d with Fig. 6a and b, it is evident how the extension of the shear walls to all the three storeys of the building produced a reduction of the maximum R_n of approximately 82% in x direction and 87% in y direction. However, it is worth noticing that this mainly confirms what is already enforced by seismic regulations, and it can be considered as a further validation of the proposed algorithm.

The above findings from stage 2 have been functional to demonstrate in retrospect the unsuitability of the design adopted for the case study building. Namely, having applied a design with discontinuous shear walls across the building's elevation in combination with the in-plan irregularity, lead to the occurrence of local vulnerabilities in the frame. This is also confirmed by the validation stage as shown in Fig. 6, which demonstrates the consistency between the post-disaster configuration of the building and the R_n variation both across the axes and storeys.

Additionally, observing the building pictures in Fig. 5a and the simulation results in Fig. 7, it is noticeable how the junction between the blocks with different elevations constitutes the most stressed portion. However, it is also the point where the most significant torsional stress occurs due to the factor highlighted above but also where the drastic change of stiffness is evidenced by a consistent displacement across the first and storeys above. Comparing therefore the results presented in Fig. 5a and b for the junction at the intersection between axes 7 in x and 1 in y directions, it is evidenced how the storeys exhibit a level of risk consistent with the effective disrupted configuration.

It is noteworthy to highlight how the second stage of this research was necessary to demonstrate the inadequacy of the layout adopted for the case-study building. In other circumstances, it is advised that the designer would extend the shear walls for the whole building's elevation to avert the risk of drastic change of rigidity, leading to soft-storey phenomena.

Having demonstrated the validity of the proposed approach, a further step was conducted over the course of Stage 3 to propose an optimized layout for the internal (LW) shear walls while preserving the layout of the façade ones (TW).

It could be argued that the chosen solution does not have shear walls in the y direction in correspondence of the junction between the building blocks. However, it has been assessed that even for the configuration analysed in Stage 2 (i.e., shear walls in their initial layout but equalling the building's elevation), the torsional deformation still occurs despite the provision of shear walls in both directions and the R_n is comparable to the one attained for 6 LW (10 shear walls in total). This stems from the adoption of a structural configuration featuring a highly irregular in-plan and in-height layout, which cannot be fully compensated with the addition of shear walls. Nonetheless, the proposed methodology led to a consistent risk reduction of more than 80% both in x and y directions as evidenced in Fig. 10.

It is worth mentioning how the adoption of the standard deviation as a parameter for the identification of the optimum solution aids the identification of the shear walls layout providing the least differential displacement across the storeys. This clearly results in preventing the occurrence of either in-plan or in-height spatial disruptions, such as the ones evidenced in the case study building. It is of paramount importance to assess both the mean value for normalized risk R_n , but at the same time the range of variability both within the storey and across the storeys (i.e., globally for the whole building) to avert the occurrence of localised vulnerabilities.

Eccentricity is also a meaningful flag for the potential occurrence of torsional phenomena, and it is clearly evidenced how the

cumulative eccentricity for the proposed solution drops to almost a fifth of its initial value, as shown in Fig. 9a.

In light of the above and considering the trend of the proposed BCR, the proposed solution presents less than half of the shear walls compared to the initial solution (10 in total) with a considerable financial benefit but also significant performance advantages.

Another consideration pertains the functionality of each solution. It is acknowledged that not all the solutions in this paper result in a floorplan providing the maximum serviceability of the environment. However, it has to be considered that this approach has been proposed in the context of a rehabilitation intervention, where an existing frame is considered and consequently the relocation of the structural grid is not allowed. However, the adoption of this methodology in earlier stages of the design would enable a leaner approach by preventing the designer from manually defining different options, with the risk of disregarding the optimum one.

Regarding the third stage of the proposed research entailing the optimization of shear walls' thickness and layout, it is observed how this can be executed independently from the former two stages. The first stage is not needed provided that the model adopted for optimization has been validated a priori. Considering for instance a design scenario, this approach could be easily integrated following to a preliminary assessment of some possible locations for shear walls. The algorithm would then provide the optimum layout and thickness for an established number of shear walls. It is observed how integrating this into a wider framework would disclose the potential to further improve the level of optimization in order to identify the optimum shear walls number.

It has been observed that Fig. 9a and b exhibit a not uniform points' density. The density of points proves to be a good indicator of how quickly the algorithm finds its convergence while carrying out the optimization process. Given the underpinning operating principles of GAs, the localised density of optimum solutions indicates the similarity of the best individuals selected by the algorithm across the different generations. Therefore, it is noticed how for the proposed solution there is an agglomeration towards the tick indicating the 400 mm thick wall.

A meaningful observation pertains the significant geometric irregularities that feature this specific building. Although shear walls can provide a significant benefit in preventing torsional behaviours and the potential occurrence of soft-storey phenomena, these results are clearly pejorative of what they could be on a geometrically regular building. As a matter of fact, building regulations generally prescribe certain limitations to the allowed shape irregularities in seismic-prone areas to avert the aforementioned phenomena. Further work could also entail the application of this methodology on a "simpler" scenario. This is likely to represent the main cause for the first storey always registering a higher risk compared to the two higher ones as it clearly accounts for most of the structural stiffness. It takes a highly refined analysis to be able to therefore redistribute the action (and remediate to the design mistakes) on the other storeys given such a consistent disparity in stiffness between the first storey and the other two. Overall, it can in fact be observed how the increase of shear walls number corresponds to a reduction in the discrepancy between the R_n across the storeys.

7. Conclusions and future work

The proposed research used a RC framed building in Old Beichuan to validate an IDR-based risk formulation and then presents an optimization strategy to improve the development of internal shear walls layout using a performance-based approach.

Overall, when observing the as-built condition, it is clear how the simulation is consistent with the disrupted scenario of the second storey exhibiting the highest damage. In fact, R_n in both x and y direction presents the highest values consistently with the torsional mechanism triggered in the second storey. It is also evident how the extension of the original shear walls layout to the whole building's height leads to a drastic reduction in R_n , as demonstrated in Section 5.2. However, this is at the expense of both functionality and cost as shown in Fig. 8, where it is evident how naturally replicating the same layout for 3 storeys would lead to a proportional financial increment. This is where the adoption of an optimization technique is of paramount importance as it leads to the same benefit of the trivial solution, but with a major reduction in the resources needed to achieve that performance level.

The advantage of decomposing the risk at the structural level into axes leads to a higher control on the different frame components and it aids a smoother identification of the most vulnerable junctions. Stemming from these considerations, the proposed formulation of risk has a twofold application:

- At the building level, it aids the identification of the junctions/structural elements most likely to undergo a certain level of damage;
- At the urban scale, it enables a weighed representation of risk which factors in the strategic importance of a specific structures, leading to an easier implementation into disaster management strategies.

The authors would like to acknowledge the following limitations that can inform further research:

- *The adoption of the GA for the optimization may lead to time-consuming analyses when using a significant number of variables. We have mitigated this by limiting the number of variables but also by targeting the population and generation features*
- Our research work utilizes a proportional approach for cost based on material quantity. This clearly does not account for all other costs related to transportation, construction, and contingencies.
- On a different note, the authors appreciate that recent research related to seismic-induced loss accounts for non-structural elements within a given building. To this respect, the authors wish to maintain that the proposed research is applicable to all those structures where the non-structural elements can be considered as part of civil works (i.e., not equipment related or requiring specific inputs from external manufacturers) and as long as these can be modelled within a structural analysis software.

These limitations will form the basis for future research, while also considering the impact of masonry infill panels.

Future work shall involve a further stage of optimization aiming at identifying the optimum amount of shear walls, benchmarked with financial and performance targets. It would be also of interest to integrate requirement for minimum room's areas into the

optimization of shear walls configuration. This could be implemented imposing specific conditions on each shear wall layout by for instance forcing the algorithm to define wall-free zone of specific minimum areas to comply with functionality or regulatory requirements.

In line with the limitations outlined above, future research would also benefit from the use of alternative algorithms other than GA. Furthermore, the results from such research could be benchmarked with the ones obtained using GA to evaluate the effectiveness of the proposed algorithms.

A further improvement would be to benchmark all the achieved solutions with more accurate cost parameters accounting for manpower, material provision and site-related costs. This could be done by perhaps automating the development of bill of quantities and adopting the resulting value as an objective for the optimization. This, combined with a functionality-related criterion as described above, would remove the likelihood for the manual process necessary to compare the solutions. Similarly, it would be relatively simple to also include the mean R_n value and the corresponding error (i.e., standard deviation) as a parameter for an expansion of this optimization work in the future.

In addition to the above, it is worth mentioning that the proposed methodology does not feature an event-specific approach. In fact, this research can be implemented on any seismic event further to gathering the motion dataset to be then implemented within the spectrum characterization.

Similarly, our research is transferrable and scalable in that it enables applications outside the scope of this paper, that could encompass broader risk assessments even not specifically linked to shear-wall optimization. This could be targeted in future research.

Finally, it should be noted that the proposed definition of risk can also be adopted in conjunction with any other performance-enhancement structural strategy as the two are not interlinked. This results in a transferrable approach which could suit applications at the urban scale as the structural intervention needs to be building-specific.

Authors' statement

All Authors involved in this research work certify to have viewed and approved the final version of the manuscript being submitted.

The Authors further warrant that the submitted research article is the Authors' original work and it has not received prior publication and it is not under consideration for publication elsewhere.

Funding

This research is supported by the Building Research Establishment (BRE) and the Natural Environment Research Council (NERC) under grant NE/N012240/1 (Resilience to earthquake-induced landslide risk in China).

Availability of data and material

Available.

Code availability

Not available.

Declaration of competing interest

The authors declare that they have no known competing financial interests or personal relationships that could have appeared to influence the work reported in this paper.

References

- [1] S. Tesfamariam, M. Saatcioglu, Risk-based seismic evaluation of reinforced concrete buildings, *Earthq. Spectra* 24 (2008) 795–821, <https://doi.org/10.1193/1.2952767>.
- [2] G. Cerè, Y. Rezgui, W. Zhao, Critical review of existing built environment resilience frameworks: directions for future research, *Int. J. Disaster Risk Reduc.* 25 (2017) 173–189, <https://doi.org/10.1016/j.ijdrr.2017.09.018>.
- [3] G. Cerè, Y. Rezgui, W. Zhao, Urban-scale framework for assessing the resilience of buildings informed by a delphi expert consultation, *Int. J. Disaster Risk Reduc.* 36 (2019) 101079, <https://doi.org/10.1016/j.ijdrr.2019.101079>.
- [4] N. Lazar, M. Dolšek, Risk-based seismic design-An alternative to current standards for earthquake-resistant design of buildings, in: *15th World Conference on Earthquake Engineering*, 2012. Lisbon.
- [5] M.C. Marulanda, M.L. Carreño, O.D. Cardona, et al., Probabilistic earthquake risk assessment using CAPRA: application to the city of Barcelona, Spain, *Nat. Hazards* 69 (2013) 59–84, <https://doi.org/10.1007/s11069-013-0685-z>.
- [6] M. Vona, A novel approach to improve the code provision based on a seismic risk index for existing buildings, *J. Build. Eng.* 28 (2020) 101037, <https://doi.org/10.1016/j.jobe.2019.101037>.
- [7] E. Cosenza, C. Del Vecchio, M. Di Ludovico, et al., The Italian guidelines for seismic risk classification of constructions: technical principles and validation, *Bull. Earthq. Eng.* 16 (2018) 5905–5935, <https://doi.org/10.1007/s10518-018-0431-8>.
- [8] Ministry of Infrastructures and Transportations, Ministerial Decree N. 58 of 28/02/2017, 2017.
- [9] Ministry of Infrastructures and Transportations, Ministerial Decree n.24 of 9/01/2020, 2020.
- [10] V. Silva, H. Crowley, M. Pagani, et al., Development of the OpenQuake engine, the Global Earthquake Model's open-source software for seismic risk assessment, *Nat. Hazards* 72 (2014) 1409–1427, <https://doi.org/10.1007/s11069-013-0618-x>.
- [11] The European Union Per Regulation 305/2011, EN 1998-1:2004+A1:2003. Eurocode 8: Design of Structures for Earthquake Resistance, 2004.
- [12] Ministry of Infrastructures and Transportations, Ministry of the Interior, Head of Department of Civil Protection, DM (Ministerial Decree) 17 January 2018. Nuove Norme Tecniche per le Costruzioni [New technical codes for constructions, 2018.].
- [13] M.J. Fadaee, D.E. Grierson, Design optimization of 3D reinforced concrete structures having shear walls, *Eng. Comput.* 14 (1998) 139–145.

- [14] Y. Zhang, C. Mueller, Shear wall layout optimization for conceptual design of tall buildings, *Eng. Struct.* 140 (2017) 225–240, <https://doi.org/10.1016/j.engstruct.2017.02.059>.
- [15] R. Vicente, S. Parodi, S. Lagomarsino, et al., Seismic vulnerability and risk assessment: case study of the historic city centre of Coimbra, Portugal, *Bull. Earthq. Eng.* 9 (2011) 1067–1096, <https://doi.org/10.1007/s10518-010-9233-3>.
- [16] United Nations Office for Disaster Risk Reduction (Unidrr) Terminology - UNDRR. <https://www.unisdr.org/we/inform/terminology>. Accessed 4 Oct 2019.
- [17] World Bank, *Kyrgyz Republic - Measuring Seismic Risk*, 2017.
- [18] A. Anelli, S. Santa-Cruz, M. Vona, et al., A proactive and resilient seismic risk mitigation strategy for existing school buildings, *Struct. Infrastruct. Eng.* 15 (2019) 137–151, <https://doi.org/10.1080/15732479.2018.1527373>.
- [19] J.A. Valcárcel, M.G. Mora, O.D. Cardona, et al., Methodology and applications for the benefit cost analysis of the seismic risk reduction in building portfolios at broadscale, *Nat. Hazards* 69 (2013) 845–868, <https://doi.org/10.1007/s11069-013-0739-2>.
- [20] I. Iervolino, A. Spillatura, P. Bazzurro, RINTC: assessing the (implicit) seismic risk of code-conforming structures in Italy, in: M. Papadrakakis, M. Fragiadakis (Eds.), 6th ECCOMAS Thematic Conference on Computational Methods in Structural Dynamics and Earthquake Engineering, Rhodes Island, Greece, 2017, pp. 1545–1557.
- [21] D. Giardini, The global seismic hazard assessment program (GSHAP) - 1992/1999, *Ann. Geofisc.* 42 (1999).
- [22] G. Fabbrocino, I. Iervolino, F. Orlando, E. Salzano, Quantitative risk analysis of oil storage facilities in seismic areas, *J. Hazard Mater.* 123 (2005) 61–69, <https://doi.org/10.1016/j.jhazmat.2005.04.015>.
- [23] R.P. Nanda, N.K. Paul, N.M. Chanu, S. Rout, Seismic risk assessment of building stocks in Indian context, *Nat. Hazards* 78 (2015) 2035–2051, <https://doi.org/10.1007/s11069-015-1818-3>.
- [24] F. Braga, F. Morelli, C. Picchi, W. Salvatore, Development of a macroseismic model for the seismic risk classification of existing buildings, in: ANIDIS. Pistoia, 2017.
- [25] European Seismological Commission, *European Macroseismic Scale: EMS-98*, 1998. Luxembourg.
- [26] S. Lagomarsino, S. Giovinazzi, Macroseismic and mechanical models for the vulnerability and damage assessment of current buildings, *Bull. Earthq. Eng.* 4 (2006) 415–443, <https://doi.org/10.1007/s10518-006-9024-z>.
- [27] Structural Engineers Association of California (Seaac), *Vision 2000: Performance Based Seismic Engineering of Buildings*, 1995. Sacramento, CA (USA).
- [28] Federal Emergency Management Agency, American Society of Civil Engineers, FEMA 356. PRESTANDARD AND COMMENTARY FOR THE SEISMIC REHABILITATION OF BUILDINGS, 2000. Washington D.C.
- [29] G.M. Calvi, T.J. Sullivan, D.P. Welch, A seismic performance classification framework to provide increased seismic resilience, in: Atila Ansal (Ed.), *Perspectives on European Earthquake Engineering and Seismology*, Springer, Cham, 2014, pp. 361–400.
- [30] Y. Dong, D.M. Frangopol, Performance-based seismic assessment of conventional and base-isolated steel buildings including environmental impact and resilience, *Earthq. Eng. Struct. Dynam.* 45 (2016) 739–756, <https://doi.org/10.1002/eqe.2682>.
- [31] D. De Domenico, G. Ricciardi, Earthquake-resilient design of base isolated buildings with TMD at basement: application to a case study, *Soil Dynam. Earthq. Eng.* 113 (2018) 503–521, <https://doi.org/10.1016/j.soildyn.2018.06.022>.
- [32] G.M. Calvi, A displacement-based approach for vulnerability evaluation of classes of buildings, *J. Earthq. Eng.* 3 (1999) 411–438, <https://doi.org/10.1080/13632469909350353>.
- [33] A. Ghobarah, On drift limits associated with different damage levels, in: P. Fajfar, H. Krawinkler (Eds.), *Performance-based Seismic Design-Concepts and Implementations*, vol. 28, Proceedings of international workshop. Bled, Slovenia, 2004, pp. 321–332.
- [34] S. Nath, N. Debnath, S. Choudhury, Effect of eccentricity on structural characteristics of a building, *J Civ Eng Environ Technol* 3 (2016) 729–732.
- [35] R.J. Balling, X. Yao, Optimization of reinforced concrete frames, *J. Struct. Eng.* 123 (1997) 193–202.
- [36] Ş. Atabay, Cost optimization of three-dimensional beamless reinforced concrete shear-wall systems via genetic algorithm, *Expert Syst. Appl.* 36 (2009) 3555–3561, <https://doi.org/10.1016/j.eswa.2008.02.004>.
- [37] A. Kaveh, P. Zakian, Optimal seismic design of Reinforced Concrete shear wall-frame structures, *KSCE J. Civ. Eng.* 18 (2014) 2181–2190, <https://doi.org/10.1007/s12205-014-0640-x>.
- [38] A. Titiksh, G. Bhatt, Optimum positioning of shear walls for minimizing the effects of lateral forces in multistorey-buildings, *Arch. Civ. Eng.* 63 (1) (2017) 151–162.
- [39] P.A. Krishnan, A. Francis, V.N. Pradeep, Effect of location of shear wall on buildings subjected to seismic loading, *IJERM* 6 (7) (2019) 34–37.
- [40] A.M. Abualreesh, A. Tuken, A. Albidah, N.A. Siddiqui, Reliability-based optimization of shear walls in RC shear wall-frame buildings subjected to earthquake loading, *Case Stud. Constr. Mater.* (2022), e00978.
- [41] G. Cerè, W. Zhao, Y. Rezzgui, Structural behavior analysis and optimization, integrating MATLAB with Autodesk Robot, in: I. Mutis, T. Hartmann (Eds.), 35th CIB W78 Conference: IT in Design, Construction, and Management, Springer, Chicago (USA), 2018, pp. 379–386.
- [42] D.B. Fogel, The advantages of evolutionary computing, in: D. Lundh, B. Olsson, A. Narayanan (Eds.), *Biocomputing and Emergent Computation: Proceedings of BCEC97*, World Scientific, 1997.
- [43] Incorporated Research Institutions for Seismology (IRIS) IRIS: Wilber 3. http://ds.iris.edu/wilber3/find_stations/2695921. Accessed 20 Jun 2019.